



# Prognostic $^{18}\text{F}$ -flotufolastat PET parameters for outcome assessment of $^{177}\text{Lu}$ -labeled PSMA-targeted radioligand therapy in metastatic castration-resistant prostate cancer

Amir Karimzadeh<sup>1,2</sup> · Kimberley Hansen<sup>1</sup> · Ergela Hasa<sup>1</sup> · Bernhard Haller<sup>3</sup> · Matthias M. Heck<sup>4</sup> · Robert Tauber<sup>4</sup> · Calogero D'Alessandria<sup>1</sup> · Wolfgang A. Weber<sup>1,5</sup> · Matthias Eiber<sup>1,5</sup> · Isabel Rauscher<sup>1</sup>

Received: 24 September 2024 / Accepted: 24 November 2024 / Published online: 23 January 2025

© The Author(s) 2024

## Abstract

**Purpose** This retrospective analysis evaluates baseline  $^{18}\text{F}$ -flotufolastat positron emission tomography (PET) parameters as prognostic parameters for treatment response and outcome in patients with metastatic castration-resistant prostate cancer (mCRPC) undergoing treatment with [ $^{177}\text{Lu}$ ]Lu-PSMA-I&T.

**Methods** A total of 188 mCRPC patients with baseline  $^{18}\text{F}$ -flotufolastat PET scans were included. Tumor lesions were semiautomatically delineated, with imaging parameters including volume-based and standardized uptake value (SUV)-based metrics. Outcome measures included prostate-specific antigen (PSA) response, PSA-progression-free survival (PSA-PFS), and overall survival (OS). Univariate and multivariate regression analyses assessed the impact of baseline imaging and pretherapeutic clinical parameters on outcome. Event time distributions were estimated with the Kaplan-Meier method, and groups were compared with log-rank tests.

**Results** Significant prognostic parameters for PSA response and PSA-PFS included log-transformed whole-body SUV-max (odds ratio (OR), 3.26, 95% confidence interval (CI), 2.01–5.55 and hazard ratio (HR), 0.51, 95% CI, 0.4–0.66; both  $p < 0.001$ ) and prior chemotherapy (OR 0.3, 95% CI, 0.12–0.72 and HR 1.64, 95% CI, 1.07–2.58;  $p = 0.008$  and  $p = 0.028$ , respectively). For OS, significant prognosticators were the following log-transformed parameters: number of lesions (HR 1.38, 95% CI, 1.24–1.53;  $p < 0.001$ ), TTV (HR 1.27, 95% CI, 1.18–1.37;  $p < 0.001$ ), and ITLV (HR 1.24, 95% CI, 1.16–1.33;  $p < 0.001$ ), with log-transformed TTV (HR 1.15, 95% CI, 1.04–1.27;  $p = 0.008$ ) remaining significant in multivariate analysis.

**Conclusion** At baseline, SUV-based  $^{18}\text{F}$ -flotufolastat PET metrics (e.g., whole-body SUVmax) serve as significant positive prognosticators for short-term outcomes (PSA response and PSA-PFS). In contrast, volume-based metrics (e.g., TTV) are significant negative prognosticators for long-term outcome (OS), in mCRPC patients treated with [ $^{177}\text{Lu}$ ]Lu-PSMA-I&T.

**Keywords** mCRPC · [ $^{177}\text{Lu}$ ]Lu-PSMA-I&T ·  $^{18}\text{F}$ -flotufolastat · PSMA · Radioligand therapy

Amir Karimzadeh and Kimberley Hansen contributed equally to this work as first author.

✉ Amir Karimzadeh  
amir.karimzadeh@uke.de

<sup>1</sup> Department of Nuclear Medicine, School of Medicine, Technical University of Munich, Munich, Germany

<sup>2</sup> Department of Diagnostic and Interventional Radiology and Nuclear Medicine, University Medical Center Hamburg-Eppendorf, Martinistr. 52, 20246 Hamburg, Germany

<sup>3</sup> Institute of AI and Informatics in Medicine, School of Medicine, Technical University of Munich, Munich, Germany

<sup>4</sup> Department of Urology, School of Medicine, Technical University of Munich, Munich, Germany

<sup>5</sup> Bavarian Cancer Research Center, Munich, Germany

## Introduction

$^{177}\text{Lu}$ -labeled prostate-specific membrane antigen (PSMA)-targeted radioligand therapy (RLT) has emerged as an established treatment option for patients with metastatic castration-resistant prostate cancer (mCRPC). Initially supported by data from compassionate use programs, subsequent phase II and III trials have confirmed the low toxicity and therapeutic efficacy of  $^{177}\text{Lu}$ -labeled PSMA-RLT, with the first agent now approved by regulatory bodies worldwide [1–6]. Substudies from both the TheraP and the VISION trials demonstrated the prognostic value of baseline [ $^{68}\text{Ga}$ ]Ga-PSMA-11 positron emission tomography (PET), showing that a higher whole-body mean standardized uptake

value (SUV<sub>mean</sub>) correlates with better treatment efficacy of [ $^{177}\text{Lu}$ ]Lu-PSMA-617 [7, 8]. These observations are supported by further analyses utilizing [ $^{68}\text{Ga}$ ]Ga-PSMA-11 PET, demonstrating that higher tumor volume and lower PSMA-ligand uptake intensity prognosticate poorer overall survival (OS) in patients treated with [ $^{177}\text{Lu}$ ]Lu-PSMA-617 [9–12]. Meanwhile, diagnostic imaging is increasingly shifting from  $^{68}\text{Ga}$ - to  $^{18}\text{F}$ -labeled PSMA-ligands due to several advantages of these compounds. These include a longer half-life and higher positron yield with lower energy, which contribute to higher diagnostic accuracy, as well as wider availability through facilitated delivery [13]. This shift has emphasized the prognostic impact of  $^{18}\text{F}$ -labeled PSMA-ligands (e.g.,  $^{18}\text{F}$ -PSMA-1007, or  $^{18}\text{F}$ -flotufolastat (formerly  $^{18}\text{F}$ -rhPSMA-7.3) for mCRPC patients undergoing  $^{177}\text{Lu}$ -labeled PSMA-RLT. In response, a recent analysis reported that baseline tumor uptake of  $^{18}\text{F}$ -PSMA-1007 PET was significantly associated with outcome in mCRPC [14]. However, to date there are no data on the prognostic impact of  $^{18}\text{F}$ -flotufolastat, which was approved by the US Food and Drug Administration in May 2023 for diagnostic imaging of patients with suspected recurrent, or primary, prostate cancer [15]. Therefore, this retrospective analysis aimed to evaluate baseline  $^{18}\text{F}$ -flotufolastat PET parameters (e.g., total tumor volume (TTV), whole-body SUV<sub>max</sub>) as potential prognostic parameters for prostate-specific antigen (PSA) response, PSA-progression-free survival (PSA-PFS) and OS in a large cohort of mCRPC patients receiving  $^{177}\text{Lu}$ -labeled PSMA-RLT.

**Table 1** Patient characteristics

Characteristic	
<b>Age (yr)</b>	74 (68–79)
<b>Time since initial diagnosis (yr)</b>	5.4 (3.4–9.5)
<b>No. of [<math>^{177}\text{Lu}</math>]Lu-PSMA-I&amp;T cycles</b>	4 (2–6)
<b>Pretherapeutic blood parameters</b>	
PSA, ng/mL ( <i>n</i> = 184)	71.5 (23.0–219.4)
LDH, U/L ( <i>n</i> = 183)	251 (215–324.5)
AP, U/L ( <i>n</i> = 182)	117 (73.3–213.3)
Hb, g/dL ( <i>n</i> = 186)	11.9 (10.4–13.1)
<b>Prior systemic therapies</b>	
Abiraterone	159 (84.6)
Enzalutamide	115 (61.2)
$^{223}\text{Ra}$	15 (8.0)
Docetaxel	131 (69.7)
Cabazitaxel	25 (13.3)
Previous chemotherapy	133 (70.7)
<b>Site of metastasis</b>	
Lymph nodes	127 (67.6)
Bone	174 (92.6)
Visceral, overall	39 (20.7)
Liver	13 (6.9)
Lung/Pleura	20 (10.6)
Adrenal	10 (5.3)
Brain	2 (1.1)
<b>Baseline <math>^{18}\text{F}</math>-flotufolastat PET parameters</b>	
Number of lesions ( <i>n</i> )	128 (41.0–239.0)
TTV, mL	394.1 (122.2–1125.9)
ITLV, mL	877.6 (255.7–2527.7)
Highest SUV <sub>max</sub>	60.6 (36.9–98.0)
Whole-body SUV <sub>max</sub>	13.9 (9.8–22.0)
Whole-body SUV <sub>mean</sub>	5.6 (4.8–7.2)
Whole-body SUV <sub>peak</sub>	9.0 (6.3–14.0)

Data are reported as median (interquartile range) or *n* (%).  $^{177}\text{Lu}$  = Lutetium-177; PSMA = prostate-specific membrane antigen; PSA = prostate-specific antigen; LDH = lactate dehydrogenase; AP = alkaline phosphatase; Hb = hemoglobin; mCRPC = metastatic castration-resistant prostate cancer;  $^{223}\text{Ra}$  = Radium-223;  $^{18}\text{F}$  = Fluorine-18; PET = positron emission tomography; TTV = total tumor volume; ITLV = intensity-weighted lesion volume; SUV<sub>max</sub> = maximum standardized uptake value; SUV<sub>mean</sub> = mean standardized uptake value; SUV<sub>peak</sub> = peak standardized uptake value

## Materials and methods

### Patients and $^{177}\text{Lu}$ -labeled PSMA-RLT

In this retrospective, single-center analysis data from patients with mCRPC undergoing [ $^{177}\text{Lu}$ ]Lu-PSMA-I&T therapy at our clinic between November 2017 and September 2021 were retrospectively reviewed. The patients received RLT with a standard activity of approximately 7.4 GBq [ $^{177}\text{Lu}$ ]Lu-PSMA-I&T at a median interval of 6 weeks. The treatment activity could be slightly adopted based on e.g. lab tests and tumor burden. Detailed patient characteristics are given in Table 1. Baseline  $^{18}\text{F}$ -flotufolastat PET scans were available for all patients. For treatment eligibility, PSMA-ligand uptake in tumor lesions had to be at least as high as the liver background. [ $^{177}\text{Lu}$ ]Lu-PSMA-I&T was prepared in accordance with good manufacturing practices and the German Medicinal Products Act (AMG § 13 2b). All patients gave written informed consent. Treatment was performed under the conditions outlined in article 37 of the Declaration of Helsinki concerning unproven

interventions in clinical practice. This retrospective analysis was approved by the institutional ethics committee (reference number 115/18S).

### PSMA-ligand PET imaging procedure

The radiolabeling of  $^{18}\text{F}$ -flotufolastat was carried out as previously described [16]. The preparation of  $^{18}\text{F}$ -flotufolastat adhered to the German Medicinal Products Act, AMG § 13 2b. All patients gave written informed consent. A mean activity of  $309 \pm 65$  MBq of  $^{18}\text{F}$ -flotufolastat (range, 89–493 MBq) was administered via intravenous bolus, with scanning initiated at a median time of 70 min (interquartile range (IQR), 65–79 min) post-injection. Patients received a diluted oral contrast medium (300 mg of Telebrix; Guerbet) and 10 mg of furosemide.  $^{18}\text{F}$ -flotufolastat PET/computed tomography (CT) was performed on a Biograph mCT Flow scanner (Siemens Medical Solutions) or a Biograph Vision scanner (Siemens Medical Solutions). PET/CT scans were acquired in 3-dimensional mode with an acquisition time of 0.8 mm/s (mCT Flow scanner) and 1.1 mm/s (Vision scanner), respectively. PET images were reconstructed using ordered-subset expectation maximization (TrueX, 4 iterations, 8 subsets) followed by a postreconstruction smoothing Gaussian filter (3 mm in full width at half maximum). A diagnostic CT scan was initially performed in the portal venous phase 80 s after intravenous injection of an iodinated contrast agent (Imeron 300; Bracco Imaging) and was followed by the PET scan.

### Baseline $^{18}\text{F}$ -flotufolastat parameters

The following imaging parameters were analyzed: number of lesions, TTV, intensity-weighted total lesion volume ( $\text{ITLV} = \sum (\text{lesion index} \times \text{lesion uptake volume})$ ), highest SUVmax, whole-body SUVmax, SUVmean, and SUVpeak. These parameters were assessed through semiautomatic delineation using aPROMISE software [17–19]. Missed pathological foci were manually added when necessary, and PSMA-avid foci resulting from physiological tracer accumulation were removed. An experienced PSMA-ligand PET reader (IR) subsequently reviewed all lesions.

### Pretherapeutic clinical parameters, PSA response and PSA-progression-free survival

The following pretherapeutic clinical parameters were assessed: age, time since initial diagnosis, prior chemotherapy, the presence of liver metastases and visceral metastases (obtained from baseline  $^{18}\text{F}$ -flotufolastat) and PSA, alkaline phosphatase (AP), lactate dehydrogenase (LDH) and hemoglobin (Hb). PSA response was defined as PSA

decline  $\geq 50\%$  from baseline according to Prostate Cancer Clinical Trials Working Group 3 [20]. PSA progression was either defined as PSA increase  $\geq 25\%$  and  $\geq 2$  ng/mL above the nadir after initial PSA decline or PSA increase  $\geq 25\%$  and  $\geq 2$  ng/mL from baseline in case with no PSA decline [20].

### Statistical analysis

Continuous covariates are reported as median values with IQR, while categorical covariates are described by their frequencies and proportions. Outcome measures are PSA response, PSA-PFS, and OS. The Kaplan-Meier method was used to estimate event time distributions, and log-rank tests were used to compare groups. Spearman's rank correlation coefficient was used to quantify strength of association between quantitative variables. A logarithmic transformation (base 2) was applied to normalize data distribution and reduce skewness for the following parameters: number of lesions, TTV, ITLV, highest SUVmax, whole-body SUVmax, SUVmean and SUVpeak, time since initial diagnosis, PSA, AP, and LDH. Univariate and multivariate logistic and Cox regression analyses were performed to assess the impact of baseline imaging and pretherapeutic clinical parameters on PSA response, PSA-PFS, and OS. Highly correlated ( $r > 0.7$ ; Supplementary Table 1) volume- and SUV-based metrics (highest SUVmax, whole-body SUVmax, and SUVmean as well as number of lesions and TTV) were included in multivariate logistic and Cox regression models and a backward variable selection procedure with a significance level of 0.05 was performed to determine the covariate(s) with the strongest association to the outcome variables. The remaining significant parameters were then included in a multivariate model together with other significant pretherapeutic clinical parameters from the univariate analyses. Whole-body SUVpeak and ITLV were excluded from this analysis due to their high correlation with whole-body SUVmax and TTV, respectively. Both indicating an almost perfect linear correlation and therefore providing no additional prognostic benefit (Supplementary Fig. 1A and B and Supplementary Table 1). Odds ratios (OR), hazard ratios (HR) and corresponding 95% confidence intervals (CI) are presented, with a  $p$ -value of  $< 0.05$  considered statistically significant. Statistical analyses were performed using GraphPad Prism version 10.2.2 (341) for Mac.

### Results

Median follow-up time was 13.3 months (IQR, 6.7–21.6 months). PSA response was achieved in 36.1% (65/180) patients. Median OS was 14.4 months (95% CI, 12.9–15.9

months) and median PSA-PFS was 4.1 months (95% CI, 3.2–5.0 months). At the time of analysis, 74.5% (140/188) patients had shown PSA progression and 86.2% (162/188) patients had deceased.

### PSA response and PSA-progression-free survival

Detailed results of univariate and multivariate logistic and Cox regression analyses for PSA response and PSA-PFS are presented in Tables 2 and 3, respectively. Baseline imaging parameters that were significant prognosticators of PSA response and PSA-PFS in the univariate analyses include the following log-transformed SUV-based metrics: highest SUV<sub>max</sub> (OR 1.85, 95% CI, 1.33–2.62 and HR 0.68, 95% CI, 0.57–0.81; both  $p < 0.001$ ), whole-body SUV<sub>max</sub> (OR 2.80, 95% CI, 1.83–4.48 and HR, 0.59, 95% CI, 0.47–0.74; both  $p < 0.001$ ), whole-body SUV<sub>mean</sub> (OR, 3.96, 95% CI, 2.0–8.33 and HR, 0.60, 95% CI, 0.42–0.86;  $p < 0.001$  and  $p = 0.006$ , respectively), and whole-body SUV<sub>peak</sub> (OR, 2.65, 95% CI, 1.71–4.25 and HR, 0.6, 95% CI, 0.47–0.76; both  $p < 0.001$ ). A stepwise backward multivariate logistic and Cox regression analysis was performed, identifying whole-body SUV<sub>max</sub> as the strongest prognosticator for both PSA response and PSA-PFS. Whole-body SUV<sub>max</sub> was then tested against all other significant pretherapeutic clinical parameters from the univariate analysis, namely age, log-transformed time since initial diagnosis, prior chemotherapy, log-transformed AP (only for PSA-PFS) and log-transformed LDH. In this multivariate analysis,

whole-body SUV<sub>max</sub> remained a significant prognosticator for PSA response (OR, 3.26, 95% CI, 2.01–5.55,  $p < 0.001$ ) and PSA-PFS (HR, 0.51, 95% CI, 0.4–0.66,  $p < 0.001$ ). Prior chemotherapy also showed significance as a prognosticator for both PSA response (OR, 0.3, 95% CI, 0.12–0.72,  $p = 0.008$ ) and PSA-PFS (HR, 1.64, 95% CI, 1.07–2.58,  $p = 0.028$ ).

### Overall survival

Detailed results for univariate and multivariate Cox regression analyses for OS are presented in Table 4. Baseline imaging parameters significantly prognostic for OS in univariate Cox regression analysis included the following log-transformed volume-based metrics: number of lesions (HR, 1.376, 95% CI, 1.24–1.533;  $p < 0.001$ ), TTV (HR, 1.271, 95% CI, 1.182–1.368;  $p < 0.001$ ), and ITLV (HR, 1.24, 95% CI, 1.158–1.329;  $p < 0.001$ ). Figure 1 presents examples of two patients with varying levels of these parameters and different outcomes. A stepwise backward Cox regression analysis was performed, including the number of lesions and TTV as candidates, which identified TTV as the stronger prognosticator for OS. When testing the prognostic value of TTV adjusting for significant pretherapeutic clinical parameters from the univariate analysis, namely log-transformed time since initial diagnosis, prior chemotherapy, the presence of liver metastases and visceral metastases, log-transformed PSA, log-transformed AP, log-transformed LDH and Hb, the following remained significant prognosticators

**Table 2** Logistic regression analysis of baseline parameters and PSA Response

Parameter	Univariate logistic regression, OR (95%CI)	<i>p</i> -value	Multiple logistic regression, OR (95%CI)	<i>p</i> -value
<b>PSMA-ligand PET parameters</b>				
Number of lesions	0.95 [0.8–1.15]	0.611		
TTV	1.02 [0.89–1.16]	0.802		
ITLV	1.05 [0.92–1.19]	0.488		
Highest SUV <sub>max</sub>	1.85 [1.33–2.62]	<b>&lt;0.001</b>		
Whole-body SUV <sub>max</sub>	2.80 [1.83–4.48]	<b>&lt;0.001</b>	3.26 [2.01–5.55]	<b>&lt;0.001</b>
Whole-body SUV <sub>mean</sub>	3.96 [2.0–8.33]	<b>&lt;0.001</b>		
Whole-body SUV <sub>peak</sub>	2.65 [1.71–4.25]	<b>&lt;0.001</b>		
<b>Pretherapeutic clinical parameters</b>				
Age	1.04 [1.0–1.08]	<b>0.035</b>	1.0 [0.95–1.06]	0.987
Time since initial diagnosis	1.38 [1.03–1.87]	<b>0.034</b>	1.31 [0.9–1.94]	0.166
Prior chemotherapy	0.33 [0.17–0.64]	<b>0.001</b>	0.3 [0.12–0.72]	<b>0.008</b>
Liver metastases	1.12 [0.32–3.49]	0.855		
Visceral metastases	0.95 [0.44–2.0]	0.890		
PSA	1.02 [0.90–1.15]	0.810		
AP	0.78 [0.58–1.03]	0.091		
LDH	0.57 [0.31–0.93]	<b>0.039</b>	0.79 [0.42–1.37]	0.435
Hb	1.15 [0.98–1.37]	0.094		

All continuous parameters except age and Hb were log (base2) transformed. Significant *p*-values are given in bold. PSA = prostate-specific antigen; OR = odds ratio; CI = confidence interval; PSMA = prostatespecific membrane antigen; PET = positron emission tomography; TTV = total tumor volume; ITLV = intensity-weighted lesion volume; SUV<sub>max</sub> = maximum standardized uptake value; SUV<sub>mean</sub> = mean standardized uptake value; SUV<sub>peak</sub> = peak standardized uptake value; AP = alkaline phosphatase; LDH = lactate dehydrogenase; Hb = hemoglobin

**Table 3** Cox Regression Analysis of Baseline Parameters and PSA-PFS

Parameter	Univariate Cox regression, HR (95%CI)	<i>p</i> -value	Multivariate Cox regression, HR (95%CI)	<i>p</i> -value
<b>PSMA-ligand PET parameters</b>				
Number of lesions	1.04 [0.93–1.15]	0.529		
TTV	0.99 [0.92–1.06]	0.722		
ITLV	0.97 [0.91–1.04]	0.436		
Highest SUV <sub>max</sub>	0.68 [0.57–0.81]	<b>&lt;0.001</b>		
Whole-body SUV <sub>max</sub>	0.59 [0.47–0.74]	<b>&lt;0.001</b>	0.51 [0.4–0.66]	<b>&lt;0.001</b>
Whole-body SUV <sub>mean</sub>	0.60 [0.42–0.86]	<b>0.006</b>		
Whole-body SUV <sub>peak</sub>	0.6 [0.47–0.76]	<b>&lt;0.001</b>		
<b>Pretherapeutic clinical parameters</b>				
Age	0.96 [0.94–0.98]	<b>&lt;0.001</b>	0.98 [0.96–1.01]	0.226
Time since initial diagnosis	0.8 [0.68–0.93]	<b>0.005</b>	0.9 [0.74–1.09]	0.266
Prior chemotherapy	1.68 [1.15–2.49]	<b>0.008</b>	1.64 [1.07–2.58]	<b>0.028</b>
Liver metastases	1.0 [0.52–1.74]	0.986		
Visceral metastases	0.80 [0.52–1.19]	0.292		
PSA	1.02 [0.96–1.09]	0.543		
AP	1.27 [1.09–1.47]	<b>0.002</b>	1.09 [0.89–1.33]	0.387
LDH	1.46 [1.18–1.76]	<b>&lt;0.001</b>	1.30 [0.98–1.69]	0.056
Hb	0.50 [0.23–1.11]	0.084		

All continuous parameters except age and Hb were log (base2) transformed. Significant *p*-values are given in bold. PSA = prostate-specific antigen; PFS = progression-free survival; HR = hazard ratio; CI = confidence interval; PSMA = prostate-specific membrane antigen; PET = positron emission tomography; TTV = total tumor volume ITLV = intensity-weighted lesion volume; SUV<sub>max</sub> = maximum standardized uptake value; SUV<sub>mean</sub> = mean standardized uptake value; SUV<sub>peak</sub> = peak standardized uptake value; AP = alkaline phosphatase; LDH = lactate dehydrogenase; Hb = hemoglobin

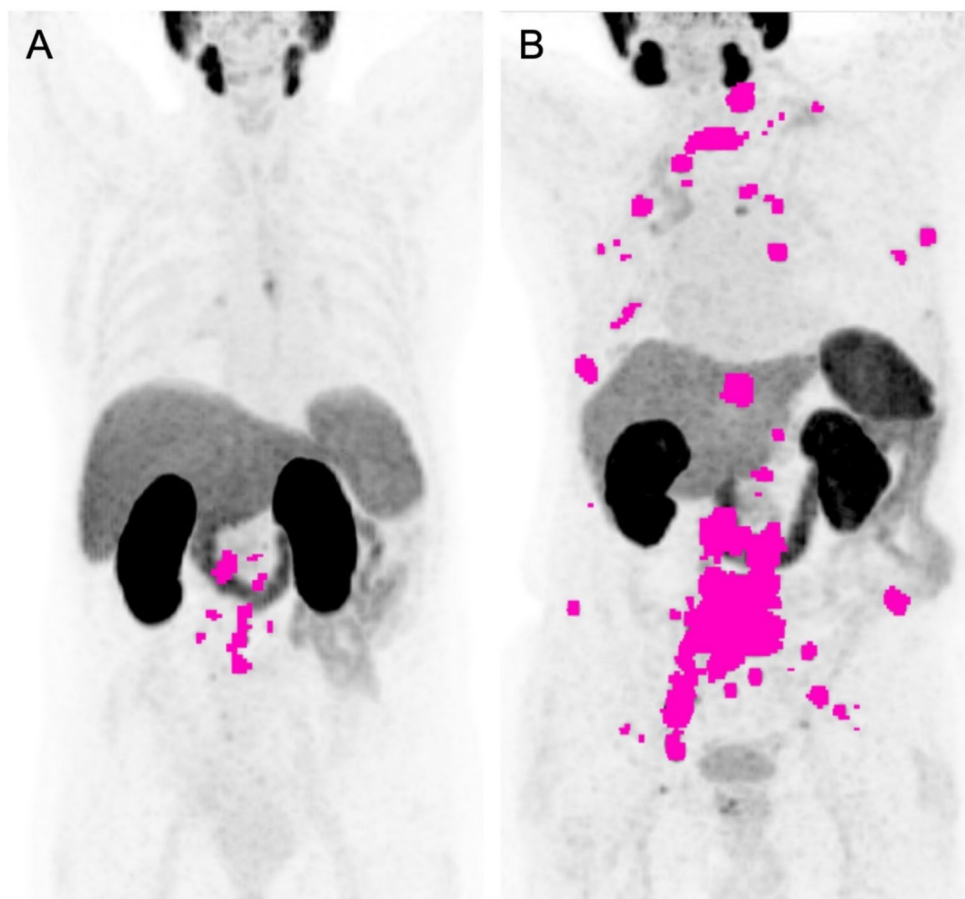
**Table 4** Cox Regression Analysis of Baseline Parameters and OS

Parameter	Univariate Cox regression, HR (95%CI)	<i>p</i> -value	Multivariate Cox regression, HR (95%CI)	<i>p</i> -value
<b>PSMA-ligand PET parameters</b>				
Number of lesions	1.38 [1.24–1.53]	<b>&lt;0.001</b>		
TTV	1.27 [1.18–1.37]	<b>&lt;0.001</b>	1.15 [1.04–1.27]	<b>0.008</b>
ITLV	1.24 [1.16–1.33]	<b>&lt;0.001</b>		
Highest SUV <sub>max</sub>	1.12 [0.97–1.29]	0.139		
Whole-body SUV <sub>max</sub>	0.96 [0.79–1.17]	0.711		
Whole-body SUV <sub>mean</sub>	0.78 [0.55–1.09]	0.148		
Whole-body SUV <sub>peak</sub>	0.98 [0.81–1.19]	0.849		
<b>Pretherapeutic clinical parameters</b>				
Age	1.0 [0.98–1.02]	0.988		
Time since initial diagnosis	0.75 [0.65–0.88]	<b>&lt;0.001</b>	0.85 [0.71–1.02]	0.089
Prior chemotherapy	1.56 [1.11–2.23]	<b>0.012</b>	1.10 [0.75–1.65]	0.63
Liver metastases	2.07 [1.05–3.68]	<b>0.021</b>	0.89 [0.41–1.83]	0.747
Visceral metastases	1.77 [1.18–2.58]	<b>0.004</b>	1.76 [1.04–2.87]	<b>0.028</b>
PSA	1.17 (1.091–1.250)	<b>&lt;0.001</b>	0.98 [0.9–1.07]	0.684
AP	1.56 (1.365–1.779)	<b>&lt;0.001</b>	1.14 (0.941–1.367)	0.173
LDH	2.21 (1.801–2.651)	<b>&lt;0.001</b>	1.42 (1.032–1.921)	<b>0.026</b>
Hb	0.7 (0.631–0.774)	<b>&lt;0.001</b>	0.86 (0.761–0.907)	<b>0.015</b>

All continuous parameters except age and Hb were log (base2) transformed. Significant *P*-values are given in bold. OS = overall survival; HR = hazard ratio; CI = confidence interval; PSMA = prostate-specific membrane antigen; PET = positron emission tomography; TTV = total tumor volume; ITLV = intensity-weighted lesion volume; SUV<sub>max</sub> = maximum standardized uptake value; SUV<sub>mean</sub> = mean standardized uptake value; SUV<sub>peak</sub> = peak standardized uptake value, PSA = prostate-specific antigen; AP = alkaline phosphatase; LDH = lactate dehydrogenase; Hb = hemoglobin



**Fig. 1** (A) A 70-year-old patient with lymph node metastases, showing 17 tumor lesions, a total tumor volume (TTV) of 31 ml, and an intensity-weighted total lesion volume (ITLV) of 55 ml. (B) A 77-year-old patient with bone metastases, showing 139 tumor lesions, a TTV of 322 ml, and an ITLV of 626 ml. PSA-PFS and OS were 5.4 months and 54.9 months for patient A, compared to 1.8 months and 12.0 months for patient B. The number of lesions, TTV, and ITLV were semiautomatically assessed, with tumor lesions shown in pink



of OS: log-transformed TTV (HR, 1.147, 95% CI, 1.038–1.271;  $p=0.008$ ), presence of visceral metastases (HR, 1.764, 95% CI, 1.038–2.874;  $p=0.028$ ), log-transformed LDH (HR, 1.421, 95% CI, 1.032–1.921;  $p=0.026$ ), and Hb (HR, 0.86, 95% CI, 0.761–0.97;  $p=0.015$ ).

### Risk stratification model

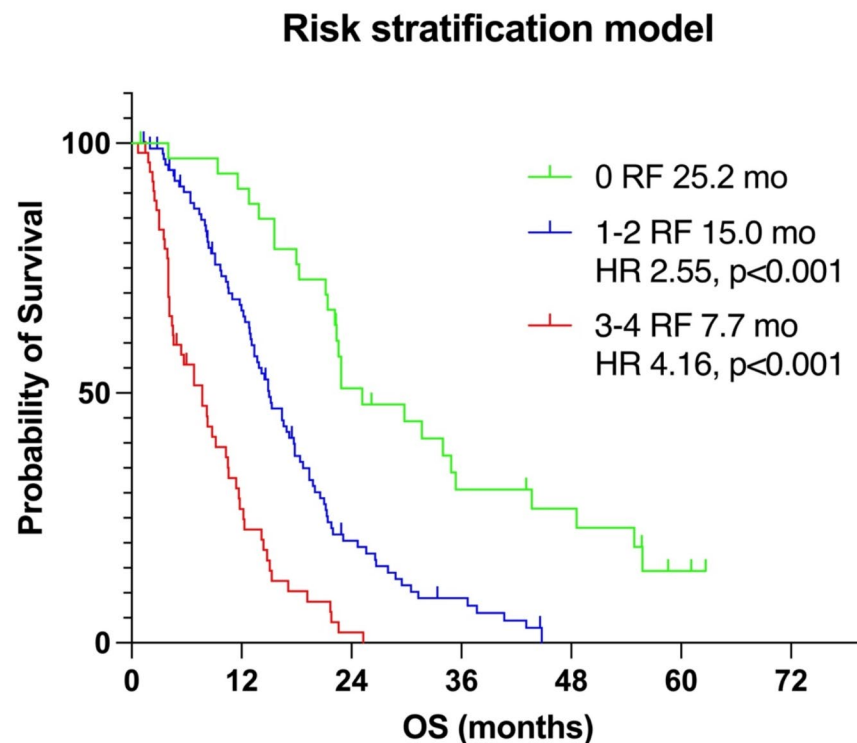
Following the approach of Hartrampf et al. [14], we propose a risk factor (RF) stratification model including all parameters that reached significance in multivariate Cox regression analysis for OS (Fig. 2). The model included high TTV ( $>394.1$  mL) and LDH levels ( $>251$  U/L) defined as values above the median, low Hb levels ( $<11.9$  g/dL) defined as values below the median, and the presence of visceral metastases, with each parameter representing one RF. Patients with no RFs had a median OS of 25.2 months. Patients with 1–2 RFs had a median OS of 15.0 months with a HR of 2.55 ( $p<0.001$ ) compared to those with 0 RFs. Patients with 3–4 RFs had a median OS of 7.7 months with an HR of 4.16 ( $p<0.001$ ) compared to those with 0 RFs.

### Discussion

SUV-based metrics in baseline  $^{18}\text{F}$ -flotufolastat PET prior to [ $^{177}\text{Lu}$ ] Lu-PSMA-I&T, including highest SUVmax, whole-body SUVmax, whole-body SUVmean, and whole-body SUVpeak, were significantly associated with PSA response and PSA-PFS in univariate analysis. Among these, whole-body SUVmax remained a significant prognosticator for both PSA response and PSA-PFS in multivariate analysis. However, these imaging parameters were not significant prognosticators of OS. In contrast, for OS, significant prognosticators included volume-based metrics such as the number of lesions, TTV, and ITLV with TTV remaining significant in multivariate analysis. The combination of imaging and pretherapeutic clinical parameters, namely TTV, the presence of visceral metastases, LDH, and Hb levels, that remained significant prognosticators of OS in multivariate analysis enabled effective stratification of patients regarding survival.

Despite the scarcity of comparative studies, our findings showed consistency with existing data on  $^{18}\text{F}$ -labeled compounds in patients with mCRPC receiving  $^{177}\text{Lu}$ -labeled PSMA-RLT. Specifically, our results confirm aspects of a recent analysis by Hartrampf et al., which explored

**Fig. 2** Kaplan-Meier survival curves for the risk stratification model, which includes baseline imaging and pretherapeutic clinical parameters that reached significance in the multivariate Cox regression analysis for OS. The model consists of the upper median values for total tumor volume (TTV) and lactate dehydrogenase (LDH) levels, the lower median value for hemoglobin (Hb), and the presence of visceral metastases. Each parameter represents one risk factor (RF). Patients were stratified based on the number of RFs: 0 RF (green line), 1–2 RFs (blue line), and 3–4 RFs (red line)



the prognostic value of baseline  $^{18}\text{F}$ -PSMA-1007 PET-derived parameters in mCRPC patients undergoing [ $^{177}\text{Lu}$ ] Lu-PSMA-I&T therapy [14]. Consistent with the prior analysis we found that volume-based metrics, such as PSMA-positive tumor volume, showed no significant impact on prognosticating PSA response [14]. We also confirm that whole-body SUVmean has a significant prognostic impact on PSA response, with a OR of 3.96 ( $p < 0.001$ ) in our analysis compared to 1.18 ( $p = 0.004$ ) in Hartrampf et al. [14]. However, due to a logarithmic transformation of SUV-based metrics in our analysis, direct comparison between the OR is not possible. Interestingly, in our analysis, log-transformed whole-body SUVmax was an even better prognosticator of PSA response (OR 2.80,  $p < 0.001$  vs. OR 1.00,  $p = 0.27$  in [14]), and it also significantly prognosticated PSA-PFS (HR 0.59,  $p < 0.001$ ). Our findings on the impact of SUV-based metrics on PSA response and PSA-PFS are also consistent with recent analyses using [ $^{68}\text{Ga}$ ] Ga-PSMA-11 PET as baseline imaging before [ $^{177}\text{Lu}$ ] Lu-labeled PSMA-RLT [7, 9, 12], further underlying their potential role in prognosticating short-term outcomes. Given that the calculation of whole-body SUVmean is more complex and depends heavily on the segmentation method, SUVmax measurements are easier to implement in clinical routine. However, SUVmax, representing the highest voxel value within the region of interest, is susceptible to image noise, which can lead to variability in measurements, particularly in small lesions,

where noise may significantly affect the maximum voxel value. Additionally, if a lesion is not precisely centered within the voxel, SUVmax may underestimate true activity, misrepresenting the lesions intensity [21]. Despite these potential drawbacks, we believe that measuring the mean SUVmax across the entire tumor burden, as represented by whole-body SUVmax, may help reduce these weaknesses and improve the reliability of SUVmax as a prognostic parameter. In contrast, SUVpeak includes a local average of SUV values from surrounding voxels, which reduces noise impact and provides a more stable, statistically reliable measurement. However, this averaging process can make SUVpeak less representative of the true activity, particularly in small lesions, compared to SUVmax. Additionally, the lack of standardization of SUVpeak across imaging protocols can result in inconsistencies in its application and interpretation [21].

While Hartrampf et al. [14] demonstrated a significant impact of whole-body SUVmean on OS (HR, 0.91;  $p = 0.03$ ), our data showed no significant association between log-transformed SUV-based metrics in general, and particularly whole-body SUVmean with OS (HR, 0.78;  $p = 0.148$ ). The positive association between whole-body SUVmean and OS has also been thoroughly reported in the context of [ $^{68}\text{Ga}$ ] Ga-PSMA-11 PET [7–10, 12]. For instance, a VISION trial substudy found that higher baseline SUVmean was associated with better OS (HR, 0.88), with the highest quartile

having an OS of 21.4 months vs. 12.6–14.6 months in the lower quartiles [8]. The median whole-body SUVmean in our cohort was 5.6 with an IQR of 4.8–7.2, indicating more homogeneous tumor uptake, which may explain the lack of correlation with OS. This reduced variability and effect size potentially reflect a narrower range of tumor differentiation, which could reduce the prognostic impact of whole-body SUVmean. However, further analyses are necessary to confirm this hypothesis and to assess the usability of SUV-based metrics in mCRPC with  $^{18}\text{F}$ -flutufolastat PET prior to  $^{177}\text{Lu}$ -labeled PSMA-RLT, especially considering the ongoing shift from  $^{68}\text{Ga}$ - to  $^{18}\text{F}$ -labeled PSMA ligands.

Our analysis shows a significant association between OS and all volume-based metrics, with TTV demonstrating significant prognostic value in multivariate analysis. These findings are in line with other retrospective analyses using [ $^{68}\text{Ga}$ ] Ga-PSMA-11 PET prior to  $^{177}\text{Lu}$ -labeled PSMA-RLT [10, 11] and comparable to the results from Seifert et al. [10], who reported a significant impact of log-transformed number of lesions (HR, 1.255;  $p=0.009$  vs. HR, 1.38;  $p<0.001$  in our analysis) and log-transformed PSMA-TV (HR, 1.299;  $p=0.005$  vs. HR, 1.27;  $p<0.001$  in our analysis). Our results underline the potential of volume-based metrics as a prognostic marker for long-term outcome.

In addition to baseline  $^{18}\text{F}$ -flutufolastat PET parameters, pretherapeutic clinical parameters significantly impacted prognosticating outcome. Prior chemotherapy was significantly associated with worse short-term outcomes like PSA response and PSA-PFS in multivariate analyses (OR, 0.3 and HR, 1.64;  $p=0.008$  and  $p=0.028$ , respectively). This association, previously reported with  $^{177}\text{Lu}$ -labeled PSMA-RLT and radiographic PFS, likely reflects the more advanced disease stage of heavily pretreated patients [12,22,23]. The same applies to the role of visceral metastases, where their presence at the start of  $^{177}\text{Lu}$ -labeled PSMA-RLT indicates more aggressive disease and poorer outcomes. Numerous retrospective analyses have shown their negative prognostic impact on OS [2, 6, 12]. Our findings also demonstrate that visceral metastases are significantly associated with poorer OS (HR, 1.76,  $p=0.028$ ). Furthermore, our results demonstrate that higher levels of log-transformed LDH and lower levels of Hb are independently associated with poorer OS (HR, 1.42;  $p=0.026$ ; and HR, 0.86;  $p=0.015$ , respectively). These associations were also reported by previous retrospective analyses [2, 6, 12], further underlying the prognostic significance of these parameters.

The combination of all significant prognostic parameters of OS from the multivariate analysis into a risk stratification model—including high tumor volume (TTV>394.1 mL), elevated lactate dehydrogenase (LDH>251 U/L), low hemoglobin (Hb<11.9 g/dL), and the presence of visceral metastases—allowed for effective stratification of

outcomes. Patients with 1–2 RFs had an approximately two times higher risk of death (HR 2.546;  $p<0.001$ ), and those with 3–4 RFs had an approximately four times higher risk of death (HR 4.161;  $p<0.001$ ) compared to those with 0 RFs. This risk stratification model demonstrates that combining risk factors identified in our multivariate analysis provides a potential tool for prognosticating outcomes.

In addition to the retrospective nature of the present analysis, this analysis has several limitations. Volume-based metrics were assessed without distinguishing the origin of lesions, which could affect outcomes. Additionally, as mentioned above, the SUVmean calculation depends on the segmentation method, unlike parameters such as SUVmax, which should be considered when comparing with other studies using different approaches (e.g., relative vs. fixed thresholding). A further limitation of this analysis is the slightly wider imaging window with a median time of 70 min post-injection compared to the 60-minute time-frame recommended by EANM guidelines [24] and the 50–70-minute window used in the Phase III LIGHTHOUSE and SPOTLIGHT studies [25,26], which could introduce minor variability in tracer uptake quantification.

## Conclusion

In conclusion, baseline  $^{18}\text{F}$ -flutufolastat PET prior to  $^{177}\text{Lu}$ -labeled PSMA-RLT demonstrated significant prognostic value for outcome. SUV-based metrics, such as whole-body SUVmax, were useful for prognosticating short-term outcome (PSA response and PSA-PFS), while volume-based metrics (e.g., TTV) showed utility for prognosticating long-term outcomes (OS).

## Abbreviations

AP	Alkaline phosphatase
CI	Confidence interval
CT	Computed tomography
Hb	Hemoglobin
HR	Hazard ratio
IQR	Interquartile range
ITLV	Intensity-weighted total lesion volume
LDH	Lactate dehydrogenase
mCRPC	Metastatic castration-resistant prostate cancer
OR	Odds ratio
OS	Overall survival
PET	Positron emission tomography
PFS	Progression-free survival
PSA	Prostate-specific antigen
PSMA	Prostate-specific membrane antigen
RF	Risk factor
RLT	Radioligand therapy



SUV Standardized uptake value  
TTV Total tumor volume

**Supplementary Information** The online version contains supplementary material available at <https://doi.org/10.1007/s00259-024-07003-2>.

**Acknowledgements** Not applicable.

**Author contributions** AK, IR: study concept and design, data acquisition, data analysis, interpretation of study results and manuscript drafting. ME, IR: substantial revision of manuscript. KH, EH, MMH, RT, CDA: data acquisition, data analysis and substantial revision of manuscript. BH: statistical analysis. WAW: interpretation of study results and substantial revision of manuscript. All authors read and approved the final manuscript.

**Funding** Open Access funding enabled and organized by Projekt DEAL.  
Nothing to disclose.

**Data availability** The datasets supporting the conclusions of this study can be made available on reasonable request.

## Declarations

**Ethics approval and consent to participate** The institutional ethics committee of the Technical University of Munich approved this retrospective analysis under the reference number 115/18S. We certify that the study was performed in accordance with the ethical standards as laid down in the 1964 Declaration of Helsinki and its later amendments or comparable ethical standards. Written informed consent was obtained from all participants.

**Consent for publication** Not applicable.

**Competing interests** ME&IR report fees from Blue Earth Diagnostics Ltd. (consultant, research funding). ME reports fees from Novartis/AAA (consultant, speaker), Telix (consultant), Bayer (consultant, research funding), RayzeBio (consultant), Point Biopharma (consultant), Eckert-Ziegler (speaker), ABX GmbH (speaker) and Janssen Pharmaceuticals (consultant, speakers bureau), Parexel (image review) and Bioclinica (image review) outside the submitted work and a patent application for rhPSMA. He and other inventors are entitled to royalties on sales of  $^{18}\text{F}$ -flotufolostat. WW reports research support from BlueEarth Diagnostics, ITM, Novartis, and Pentixapharm. He has also acted as consultant for these companies. WW is an Associate Editor of EJNMML. RT: Advisory boards, speaking fees; travel support, conference access; author fees; shares: Astellas, AstraZeneca, Bayer, BMS, Eisai, EUSA, Ipsen, Janssen, Merck, MSD, Novartis, Orion, Philogen, Roche, Sanofi, Thieme. No other potential conflicts of interest relevant to this article exist.

**Open Access** This article is licensed under a Creative Commons Attribution 4.0 International License, which permits use, sharing, adaptation, distribution and reproduction in any medium or format, as long as you give appropriate credit to the original author(s) and the source, provide a link to the Creative Commons licence, and indicate if changes were made. The images or other third party material in this article are included in the article's Creative Commons licence, unless indicated otherwise in a credit line to the material. If material is not included in the article's Creative Commons licence and your intended use is not permitted by statutory regulation or exceeds the permitted

use, you will need to obtain permission directly from the copyright holder. To view a copy of this licence, visit <http://creativecommons.org/licenses/by/4.0/>.

## References

1. Rahbar K, Schmidt M, Heinzel A, et al. Response and tolerability of a single dose of  $^{177}\text{Lu}$ -PSMA-617 in patients with metastatic castration-resistant prostate cancer: a multicenter retrospective analysis. *J Nucl Med*. 2016;57:1334–8.
2. Heck MM, Tauber R, Schwaiger S, et al. Treatment outcome, toxicity, and predictive factors for radioligand therapy with  $^{177}\text{Lu}$ -PSMA-I&T in metastatic castration-resistant prostate cancer. *Eur Urol*. 2019;75:920–6.
3. Hofman MS, Violet J, Hicks RJ, et al. [ $^{177}\text{Lu}$ ]-PSMA-617 radionuclide treatment in patients with metastatic castration-resistant prostate cancer (LuPSMA trial): a single-centre, single-arm, phase 2 study. *Lancet Oncol*. 2018;19:825–33.
4. Hofman MS, Emmett L, Sandhu S, et al. [ $^{177}\text{Lu}$ ]-PSMA-617 versus cabazitaxel in patients with metastatic castration-resistant prostate cancer (TheraP): a randomised, open-label, phase 2 trial. *Lancet*. 2021;397:797–804.
5. Sartor O, de Bono J, Chi KN, et al. Lutetium-177-PSMA-617 for metastatic castration-resistant prostate cancer. *N Engl J Med*. 2021;385:1091–103.
6. Karimzadeh A, Heck M, Tauber R, et al.  $^{177}\text{Lu}$ -PSMA-I&T for treatment of metastatic castration-resistant prostate cancer: prognostic value of scintigraphic and clinical biomarkers. *J Nucl Med*. 2023;64:402–9.
7. Buteau JP, Martin AJ, Emmett L, et al. PSMA and FDG-PET as predictive and prognostic biomarkers in patients given [ $^{177}\text{Lu}$ ]-PSMA-617 versus cabazitaxel for metastatic castration-resistant prostate cancer (TheraP): a biomarker analysis from a randomised, open-label, phase 2 trial. *Lancet Oncol*. 2022;23:1389–97.
8. Kuo PH, Morris MJ, Hesterman J, et al. Quantitative  $^{68}\text{Ga}$ -PSMA-11 PET and clinical outcomes in metastatic castration-resistant prostate cancer following  $^{177}\text{Lu}$ -PSMA-617 (VISION trial). *Radiology*. 2024;312:e233460.
9. Seifert R, Seitzer K, Herrmann K, et al. Analysis of PSMA expression and outcome in patients with advanced prostate cancer receiving  $^{177}\text{Lu}$ -PSMA-617 radioligand therapy. *Theranostics*. 2020;10:7812–20.
10. Ferdinandus J, Violet J, Sandhu S, et al. Prognostic biomarkers in men with metastatic castration-resistant prostate cancer receiving [ $^{177}\text{Lu}$ ]-PSMA-617. *Eur J Nucl Med Mol Imaging*. 2020;47:2322–7.
11. Seifert R, Kessel K, Schlack K, et al. PSMA PET total tumor volume predicts outcome of patients with advanced prostate cancer receiving [ $^{177}\text{Lu}$ ]-PSMA-617 radioligand therapy in a bicentric analysis. *Eur J Nucl Med Mol Imaging*. 2021;48:1200–10.
12. Gafita A, Calais J, Grogan TR, et al. Nomograms to predict outcomes after  $^{177}\text{Lu}$ -PSMA therapy in men with metastatic castration-resistant prostate cancer: an international, multicentre, retrospective study. *Lancet Oncol*. 2021;22:1115–25.
13. Werner RA, Derlin T, Lapa C, et al.  $^{18}\text{F}$ -labeled, PSMA-targeted radiotracers: leveraging the advantages of radiofluorination for prostate cancer molecular imaging. *Theranostics*. 2020;10:1–16.
14. Hartkamp PE, Hüttmann T, Seitz AK, et al.  $\text{SUV}_{\text{mean}}$  on baseline [ $^{18}\text{F}$ ]-PSMA-1007 PET and clinical parameters are associated with survival in prostate cancer patients scheduled for [ $^{177}\text{Lu}$ ]-PSMA I&T. *Eur J Nucl Med Mol Imaging*. 2023;50:3465–74.
15. Highlights of prescribing information: POSLUMA (flotufolostat F 18) injection US Food and Drug Administration. In: <https://www>

- [w.accessdata.fda.gov/drugsatfda\\_docs/label/2023/216023s000lbl.pdf](https://www.accessdata.fda.gov/drugsatfda_docs/label/2023/216023s000lbl.pdf).
16. Wurzer A, Di Carlo D, Schmidt A, et al. Radiohybrid ligands: a novel tracer concept exemplified by  $^{18}\text{F}$ - or  $^{68}\text{Ga}$ -labeled rhPSMA inhibitors. *J Nucl Med.* 2020;61:735–742.
  17. Nickols N, Anand A, Johnsson K, et al. aPROMISE: a novel automated PROMISE platform to standardize evaluation of tumor burden in  $^{18}\text{F}$ -DCFPyL images of veterans with prostate cancer. *J Nucl Med.* 2022;63:233–239.
  18. Johnsson K, Brynolfsson J, Sahlstedt H, et al. Analytical performance of aPROMISE: automated anatomic contextualization, detection, and quantification of [ $^{18}\text{F}$ ]DCFPyL (PSMA) imaging for standardized reporting. *Eur J Nucl Med Mol Imaging.* 2022;49:1041–1051.
  19. Eiber M, Herrmann K, Calais J, et al. Prostate Cancer Molecular Imaging Standardized Evaluation (PROMISE): proposed miTNM classification for the interpretation of PSMA-ligand PET/CT. *J Nucl Med.* 2018;59:469–478.
  20. Scher HI, Morris MJ, Stadler WM, et al. Trial design and objectives for castration-resistant prostate cancer: updated recommendations from the Prostate Cancer Clinical Trials Working Group 3. *J Clin Oncol.* 2016;34:1402–1418.
  21. Adams MC, Turkington TG, Wilson JM, Wong TZ. A systematic review of the factors affecting accuracy of SUV measurements [published correction appears in *AJR Am J Roentgenol.* 2010 Oct;195:1043]. *AJR Am J Roentgenol.* 2010;195:310–320.
  22. Gafita A, Heck MM, Rauscher I, et al. Early prostate-specific antigen changes and clinical outcome after  $^{177}\text{Lu}$ -PSMA radionuclide treatment in patients with metastatic castration-resistant prostate cancer. *J Nucl Med.* 2020;61:1476–1483.
  23. Barber TW, Singh A, Kulkarni HR, Niepsch K, Billah B, Baum RP. Clinical outcomes of  $^{177}\text{Lu}$ -PSMA radioligand therapy in earlier and later phases of metastatic castration-resistant prostate cancer grouped by previous taxane chemotherapy. *J Nucl Med.* 2019;60:955–962.
  24. Fendler WP, Eiber M, Beheshti M, et al. PSMA PET/CT: joint EANM procedure guideline/SNMMI procedure standard for prostate cancer imaging 2.0. *Eur J Nucl Med Mol Imaging.* 2023;50:1466–1486.
  25. Surasi DS, Eiber M, Maurer T, et al. Diagnostic Performance and Safety of Positron Emission Tomography with 18 F-rhPSMA-7.3 in Patients with Newly Diagnosed Unfavourable Intermediate- to Very-high-risk Prostate Cancer: Results from a Phase 3, Prospective, Multicentre Study (LIGHHOUSE). *Eur Urol.* 2023;84:361–370.
  26. Jani AB, Ravizzini GC, Gartrell BA, et al. Diagnostic Performance and Safety of 18 F-rhPSMA-7.3 Positron Emission Tomography in Men With Suspected Prostate Cancer Recurrence: Results From a Phase 3, Prospective, Multicenter Study (SPOT-LIGHT). *J Urol.* 2023;210:299–311.

**Publisher's note** Springer Nature remains neutral with regard to jurisdictional claims in published maps and institutional affiliations.

## Terms and Conditions

Springer Nature journal content, brought to you courtesy of Springer Nature Customer Service Center GmbH (“Springer Nature”).

Springer Nature supports a reasonable amount of sharing of research papers by authors, subscribers and authorised users (“Users”), for small-scale personal, non-commercial use provided that all copyright, trade and service marks and other proprietary notices are maintained. By accessing, sharing, receiving or otherwise using the Springer Nature journal content you agree to these terms of use (“Terms”). For these purposes, Springer Nature considers academic use (by researchers and students) to be non-commercial.

These Terms are supplementary and will apply in addition to any applicable website terms and conditions, a relevant site licence or a personal subscription. These Terms will prevail over any conflict or ambiguity with regards to the relevant terms, a site licence or a personal subscription (to the extent of the conflict or ambiguity only). For Creative Commons-licensed articles, the terms of the Creative Commons license used will apply.

We collect and use personal data to provide access to the Springer Nature journal content. We may also use these personal data internally within ResearchGate and Springer Nature and as agreed share it, in an anonymised way, for purposes of tracking, analysis and reporting. We will not otherwise disclose your personal data outside the ResearchGate or the Springer Nature group of companies unless we have your permission as detailed in the Privacy Policy.

While Users may use the Springer Nature journal content for small scale, personal non-commercial use, it is important to note that Users may not:

1. use such content for the purpose of providing other users with access on a regular or large scale basis or as a means to circumvent access control;
2. use such content where to do so would be considered a criminal or statutory offence in any jurisdiction, or gives rise to civil liability, or is otherwise unlawful;
3. falsely or misleadingly imply or suggest endorsement, approval, sponsorship, or association unless explicitly agreed to by Springer Nature in writing;
4. use bots or other automated methods to access the content or redirect messages
5. override any security feature or exclusionary protocol; or
6. share the content in order to create substitute for Springer Nature products or services or a systematic database of Springer Nature journal content.

In line with the restriction against commercial use, Springer Nature does not permit the creation of a product or service that creates revenue, royalties, rent or income from our content or its inclusion as part of a paid for service or for other commercial gain. Springer Nature journal content cannot be used for inter-library loans and librarians may not upload Springer Nature journal content on a large scale into their, or any other, institutional repository.

These terms of use are reviewed regularly and may be amended at any time. Springer Nature is not obligated to publish any information or content on this website and may remove it or features or functionality at our sole discretion, at any time with or without notice. Springer Nature may revoke this licence to you at any time and remove access to any copies of the Springer Nature journal content which have been saved.

To the fullest extent permitted by law, Springer Nature makes no warranties, representations or guarantees to Users, either express or implied with respect to the Springer nature journal content and all parties disclaim and waive any implied warranties or warranties imposed by law, including merchantability or fitness for any particular purpose.

Please note that these rights do not automatically extend to content, data or other material published by Springer Nature that may be licensed from third parties.

If you would like to use or distribute our Springer Nature journal content to a wider audience or on a regular basis or in any other manner not expressly permitted by these Terms, please contact Springer Nature at

[onlineservice@springernature.com](mailto:onlineservice@springernature.com)